Title
Valence bands, oxygen in planes and chains, and surface changes for single crystals of M2CuO4 and MBa2Cu3Ox (M=Pr,Nd,Eu,Gd)

Journal
Physical Review B, 38(7)

ISSN
2469-9950

Authors
Weaver, JH
Meyer, HM
Wagener, TJ
et al.

Publication Date
1988-09-01

DOI
10.1103/physrevb.38.4668

Valence bands, oxygen in planes and chains, and surface changes for single crystals of M_2CuO_4 and $MBa_2Cu_3O_x$ (M = Pr, Nd, Eu, Gd)

J. H. Weaver, H. M. Meyer III, T. J. Wagener, D. M. Hill, and Y. Gao
Department of Chemical Engineering and Materials Science, University of Minnesota, Minneapolis, Minnesota 55455

D. Peterson, Z. Fisk, and A. J. Arko
Los Alamos National Laboratory, Los Alamos, New Mexico 87545
(Received 9 May 1988)

X-ray photoemission results for single crystals of M_2CuO_4 (M = Pr, Eu, Gd), $MBa_2Cu_3O_x$ (M = Nd, Gd), and CuO and sintered $La_{1.85}Sr_{0.15}CuO_4$ and $YBa_2Cu_3O_{6.9}$ show valence-band spectra within 10 eV of the Fermi energy that are remarkably similar in appearance, with contributions that reflect Cu-O hybrid states and the rare-earth $4f$ states. For Pr_2CuO_4 and $NdBa_2Cu_3O_x$, there are two distinct $4f$ features due to ligand screening in the photoemission final state. The rare-earth $5p$ core-level emission overlaps the O $2s$ emission and reveals complex $5p$-$4f$ multiplet interactions. All O $1s$ spectra show a dominant peak at $\sim$528 eV that can be resolved into features separated by $\sim$0.7 eV. These reflect inequivalent oxygen bonding configurations in the lattice and are associated with the planes and chains for the 1:2:3 compounds and the planes and off-planes for the 2:1:4 compounds. The lower-binding-energy feature is associated with the Cu-O chains of the 1:2:3 compounds and the Cu-O planes of the 2:1:4 compounds. In addition to the O $1s$ main line for the Cu-O planes there is also a weak satellite. Time-dependent studies of the Cu $2p$ and O $1s$ emission indicate surface modification, dependent upon the quality of the cleave. The effects of surface changes and the presence of imperfections are discussed in the context of surface studies and surface superconductivity.

INTRODUCTION

In the search for the mechanisms responsible for high-temperature superconductivity, a large number of theoretical and experimental studies of the electronic structures have been presented.[1] Photoemission and inverse photoemission have provided "benchmarks" for comparison of the energy bands and the density of states calculated within the independent particle approximation, even though the importance of correlation effects is recognized.[2,3] These experimental results have shown, for example, that the photoemission intensity near the Fermi level E_F is small, that the emission from the manifold of Cu-O hybrid states is practically indistinguishable for $La_{1.85}Sr_{0.15}CuO_4$ and $YBa_2Cu_3O_{6.9}$, and that the empty states of La, Y, and Ba can be readily identified. The band calculations have suggested a somewhat higher density of states near E_F and indicate greater differences in the electronic structure of the 2:1:4 and 1:2:3 materials.

In the photoemission results, the O $1s$ core-level spectra have been the source of controversy, especially for the 1:2:3 materials. It has generally been thought that inequivalent O sites in the unit cell might give rise to resolvable O $1s$ features. At the same time, it has also been proposed that O $1s$ final-state screening effects might give rise to multiple features,[4] analogous to those associated with Cu $2p$ and $3d$ emission, and these might offer critical insight into Cu—O bonding. Until recently, these issues have been difficult to address because photoemission spectra for sintered, polycrystalline samples were generally troubled by multiple bulk phases, grain boundary phases, or contamination, all of which introduce emission from spurious O bonding configurations.[1]

In this paper, we report x-ray photoemission results for single crystals of the rare-earth copper oxides M_2CuO_4 (M = Pr, Eu, Gd) and $MBa_2Cu_3O_x$ (M = Nd and Gd), together with single-crystal CuO and clean, polycrystalline samples of $La_{1.85}Sr_{0.15}CuO_4$ and $YBa_2Cu_3O_{6.9}$ (from Ref. 1). The goal of these studies was to compare the electronic structures of the 1:2:3 and 2:1:4 materials, to examine in detail the valence-band differences associated with substitution of rare-earth ions for La or Y, and to identify the intrinsic and extrinsic O $1s$ features. We were able to distinguish oxygen atoms in the Cu-O planes and chains and to observe a weaker $1s$ satellite. Cu $2p$ and O $1s$ time dependences were used to show variations in stoichiometry and order for some of these samples.

EXPERIMENT

Single crystals of the 2:1:4 superconductors and $NdBa_2Cu_3O_x$ were grown from PbO-based fluxes in air. The $GdBa_2Cu_3O_x$ single crystals were grown in flowing oxygen by slow cooling a flux containing 10 at.% Gd_2O_3, 30 at.% BaO_2, and 60 at.% CuO. These crystals were mechanically removed from the frozen eutectic matrix. The Pr_2CuO_4, Eu_2CuO_4, and Gd_2CuO_4 crystals were undoped and crystallized in a tetragonal structure related to the K_2NiF_4 structure but in which the oxygen atoms out of the Cu-O planes are rotated from 45° about the z axis.

The $NdBa_2Cu_3O_x$ and $GdBa_2Cu_3O_x$ single crystals were tetragonal with x values close to 6 and were semiconducting. The CuO single crystals (generously made available by C. Gallo) were grown as a by-product during synthesis of $YBa_2Cu_3O_x$, were Ba doped, and were in the form of long needles with orthogonal faces. The polycrystalline samples had transition temperatures of ~35 K and ~95 K for $La_{1.85}Sr_{0.15}CuO_4$ and $YBa_2Cu_3O_{6.9}$, respectively, and were obtained from D. Capone of Argonne National Laboratory (see Ref. 1).

The single-crystal samples were mounted with conducting epoxy onto holders and were then covered with a bead of epoxy. The single crystals were cleaved (or fractured) *in situ* by prying off the epoxy bead, thereby exposing interior surfaces. The CuO needles were cleaved to expose specular surfaces. All of the measurements were conducted at room temperature at pressures of $\sim 5\times10^{-11}$ Torr. X-ray photoemission experiments were started within 10 min of cleaving. They emphasized the valence bands, the shallow core levels within 45 eV of E_F, the O 1s, the Cu $2p_{3/2}$, and the rare-earth 4d core levels. For these measurements, the x-ray beam size was 300 μm and the pass energy of the hemispherical analyzer was 50 eV (Surface Sciences Instruments Small Spot SSX-100-3). Simultaneous inspection of the sample surface with a 50× optical microscope made it possible to position the sample in the x-ray beam and to relate spectral variations to sample topography (flat regions versus irregular features). Variations were found in the O 1s emission, as we will show, but the best spectral features were found for surfaces that had relatively large numbers of steps and broad terraces (scanning electron microscopy investigations revealed terraces that were typically ~10 μm wide). Although we show best case results, it is possible that we were never able to obtain a surface which was completely free of emission from an impurity oxygen configuration. Since the samples were grown from the melt, small amounts of flux could be incorporated. The tendency of the crystals to fracture at cracks or inclusions would then expose impurities. Optical microscopy *ex situ* showed irregularities, even for surfaces which were nominally specular. In x-ray photoemission spectroscopy (XPS), no carbon 1s emission was observed for $La_{1.85}Sr_{0.15}CuO_4$ or Pr_2CuO_4. For $YBa_2Cu_3O_{6.9}$ and $NdBa_2Cu_3O_x$, the C 1s photoemission intensity was less than 2 at.%. For the Gd- and Eu-containing samples, the C 1s emission overlapped with the rare-earth 4p emission but no distinguishable amount was observed.

Synchrotron radiation photoemission studies were also undertaken with Pr_2CuO_4 to resonantly enhance the Pr 4f emission in the valence bands and to examine the Cu d^8 satellites. In those studies, monochromatic photons were obtained from the Aladdin storage ring at the Wisconsin Synchrotron Radiation Center, using the facility's Grasshopper Mark V monochromator and beamline ($40 \leq h\nu \leq 150$ eV). The sample was mounted on a long, small-diameter rod so that only the sample surface was illuminated after it was cleaved. In this set of measurements, we were unable to investigate the O 1s emission and the focused photon beam flooded the 2×2 mm^2 cleaved surface.

RESULTS AND DISCUSSION

Valence bands

In Figs. 1 and 2, we show photoemission spectra for the shallow core levels and the valence bands for these 1:2:3 and 2:1:4 single crystals, together with results for polycrystalline $YBa_2Cu_3O_{6.9}$ and $La_{1.85}Sr_{0.15}CuO_4$ at the bottom of the respective figures. The binding energies are referenced to the known Fermi level of the spectrometer. As can be seen, there is low emission near E_F for all of these materials. Structure in the occupied state emission between E_F and ~8 eV reflects the Cu-O derived states. The ground-state character of these hybrid states has been identified by the various band calculations,[5,6] and deviations from the independent-particle picture are attributed to correlation or final-state effects.[2,3] To directly compare the XPS valence-band spectra for the 1:2:3 and 2:1:4 compounds, we have superimposed the results for $La_{1.85}Sr_{0.15}CuO_4$ (dashed line) with those for $YBa_2Cu_3O_{6.9}$, as shown at the bottom of Fig. 1. To do this, the energy scale for $La_{1.85}Sr_{0.15}CuO_4$ was offset to the right by 0.3 eV, aligning the leading edge of the dominant Cu-O manifold and taking into account variations in the position of E_F within the antibonding, low-density Cu-O bands. The striking similarities in the spectral

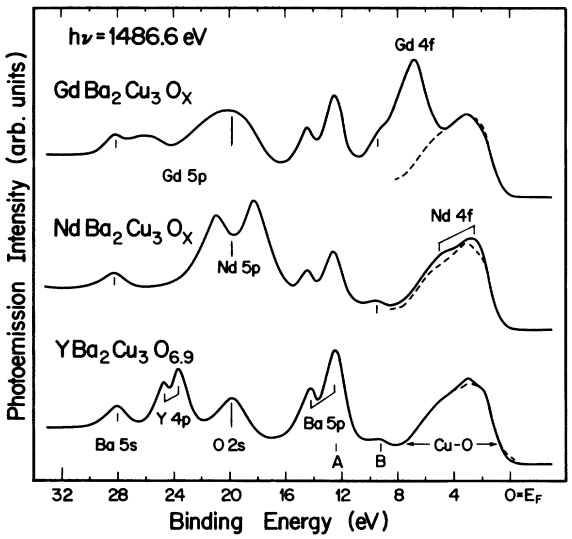

FIG. 1. Comparison of x-ray photoemission spectra for semiconducting, low-x single crystals of $GdBa_2Cu_3O_x$ and $NdBa_2Cu_3O_x$, together with polycrystalline $YBa_2Cu_3O_{6.9}$ (from Ref. 1). Comparison is facilitated by superimposing the $YBa_2Cu_3O_{6.9}$ spectrum (dashed) on the single-crystal results. In turn, the dashed curve under $YBa_2Cu_3O_{6.9}$ facilitates comparison to $La_{1.85}Sr_{0.15}CuO_4$ (from Fig. 2). In all cases, the Fermi energy is the reference but the dashed curves have been offset to align the leading edge of the Cu-O emission. The Nd 4f emission appears as a doublet because of final-state screening and the Gd 4f multiplets fall between 6 and 10 eV. Feature A reflects a Cu d^8 satellite. The origin of feature B continues to be elusive. The Nd and Gd 5p features overlap with O 2s emission (vertical line at 20 eV) and are complicated by 5p-4f multiplets.

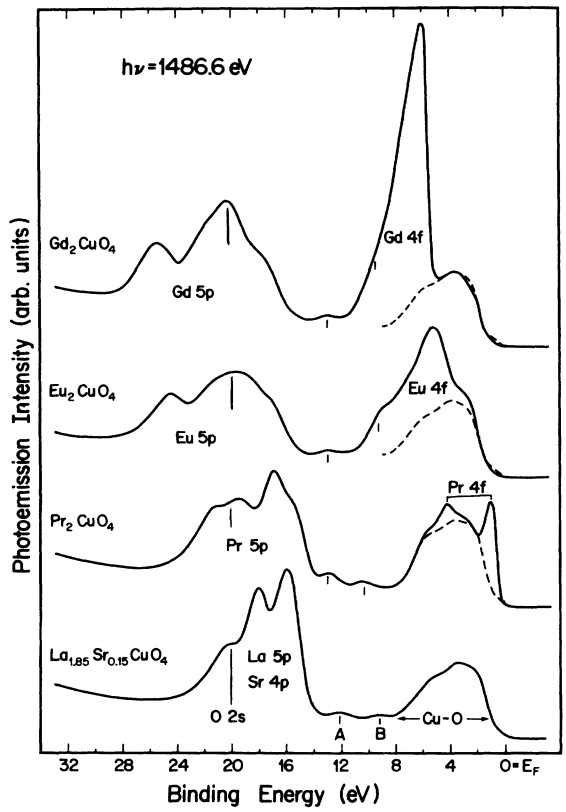

FIG. 2. XPS results for the 2:1:4 compounds analogous to those of Fig. 1. The dashed line superimposed on the single-crystal results reproduces the $La_{1.85}Sr_{0.15}CuO_4$ spectrum and makes it possible to identify the $4f$ emission of Pr, Eu, and Gd. The $4f$ and $5p$ emission is more pronounced than in Fig. 1 because of the larger number of rare-earth atoms in the 2:1:4 structure.

features for these two classes of superconductors are then evident. Indeed, the only significant difference is from enhanced emission at 3 eV for $YBa_2Cu_3O_{6.9}$ (see Ref. 1 for a detailed discussion of these results, together with results for the empty electronic states obtained by inverse photoemission and the calculated densities of states by many groups).

In Figs. 1 and 2, we compare the XPS results for the 1:2:3 and 2:1:4 families by superimposing spectra for $YBa_2Cu_3O_{6.9}$ or $La_{1.85}Sr_{0.15}CuO_4$ on those for the single crystals, again offsetting the leading edge of the "standard" spectra while keeping the Fermi level as the reference energy. From these results, we conclude that the valence bands can be well represented by a relatively invariant Cu-O manifold, with common final-state effects and with small variations in energy to account for the movement of E_F. The substitution of rare-earth ions for Y or La introduces new structures associated with the $4f$ levels, as will be discussed in the next section, and these can be easily identified.

The vertical lines at -20 eV in Figs. 1 and 2 draw attention to structure associated with O $2s$ emission. For the 1:2:3 materials of Fig. 1, there is also the Ba $5p_{1/2,3/2}$ doublet (12.5 and 14.2 eV for $YBa_2Cu_3O_{6.9}$) and Ba $5s$ emission centered at 28 eV. For the samples containing rare earths, there is emission from the $5p$ levels which shift to greater binding energy with increasing atomic number. Detailed line-shape decomposition is frustrated by the overlap of the rare-earth $5p$ and oxygen $2s$ emission. Moreover, the $5p$ emission is likely to reflect $5p$-$4f$ multiplet coupling of the sort observed in other rare-earth systems.[7,8] This coupling would account for the leading shoulder at 15–17 eV for the 2:1:4's and structure which cannot be described as a spin-orbit-split doublet. We note that nearly identical $5p$ spectral shapes were obtained for single crystals of Pr_2CuO_4 using XPS energies, with maximum bulk sensitivity, and with synchrotron radiation, with very high surface sensitivity. This suggests that the complex line shape is not a consequence of the surface (e.g., surface core-level shifts). Finally, the $4d$ core-level spectra for the rare earths (not shown) also exhibit complex line shapes because of $4d$-$4f$ multiplets, as discussed in Refs. 7 and 8.

In Fig. 3 we show the XPS valence-band spectra for Ba-doped single-crystal CuO and, for comparison, repeat the spectra for $La_{1.85}Sr_{0.15}CuO_4$ and $YBa_2Cu_3O_{6.9}$. CuO exhibits a triangular band of states centered at -4 eV which reflects Cu-O hybrid states. At higher energy, there are ^1G and ^3F final-state multiplet structures of the d^8 configuration at 12.5 and 10.3 eV, as discussed by

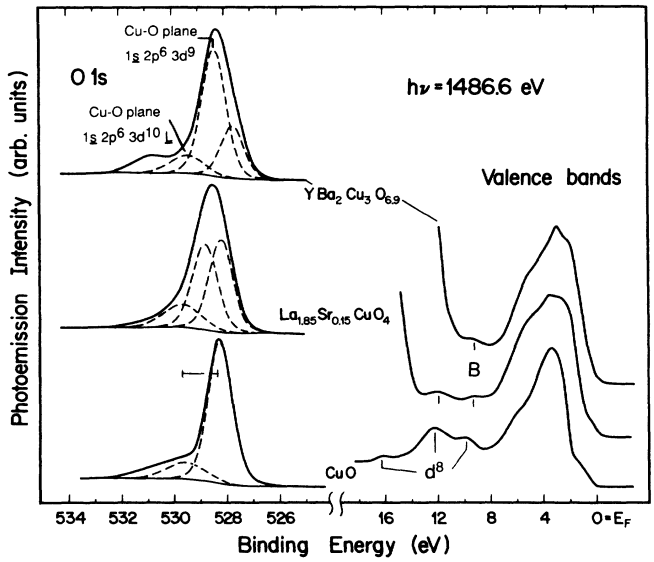

FIG. 3. Comparison of valence-band spectra for CuO, $La_{1.85}Sr_{0.15}CuO_4$, and $YBa_2Cu_3O_{6.9}$ to show the overall similarities. The Cu d^8 final-state multiplets are clearly visible because of the simple background. Feature B, which is visible in the superconductor results, may be masked by the Cu multiplets in CuO. Oxygen $1s$ core-level results shown at the left make it possible to identify the main line (O $1\underline{s}2p^63d^9$) and satellite structure (O $1\underline{s}2p^63d^{10}\underline{L}$) for CuO; this spectrum is offset 1.15 eV to simplify visible comparison (horizontal bar). O $1s$ line-shape fitting for the superconductors, based on the CuO line shape, reveals emission from Cu-O planes (shallowest for the 2:1:4's) and from O atoms coordinated with La. For the 1:2:3 structure, the large line reflects Cu-O planes and the line at lower binding energy is due to Cu-O chains. The ratio of the main line to the satellite can be used to identify the ground-state mixing of the two configurations, as discussed in the text.

Thuler, Benbow, and Hurych[9] and van der Laan *et al.*[10] For CuO, these multiplet configurations, and another at 16.6 eV, are readily identified because there is no overlapping structure. For the superconductors, the 12-eV satellite structure is labeled as *A* in Figs. 1 and 2. The shallower, weaker satellite overlaps with a stronger feature at ~9 eV (next paragraph) and the 16-eV satellite is obscured.

12-eV satellite and the 9-eV structure

Feature *A* identified by the tic marks in Figs. 1 and 2 cannot be described within the independent particle picture. However, it can be accounted for by considering Cu-O clusters [e.g., the $(CuO_6)^{10-}$ cluster used by Fujimori *et al.*[2] to model the tilelike Cu-O planes and chains of the superconductors or CuO]. Early work by Sawatsky and co-workers[10] found analogous structure in the Cu dihalides. In these systems, the excitation of a *d* electron from the ground state can form the d^8 final-state configuration with two highly correlated 3*d* holes at a Cu site, denoted d^8, or the $d^9\underline{L}$ and $d^{10}\underline{L}^2$ configurations which are reflected by the dominant valence-band emission ($\underline{L}$ corresponds to a suitably symmetrized ligand hole). Fujimori *et al.*,[2] Shen *et al.*,[3] and others have used the energy positions of these features to calculate the Coulomb (Hubbard) correlation energy of $U_{3d\,3d} \cong 6$ eV for $YBa_2Cu_3O_x$ and $La_{1.85}Sr_{0.15}CuO_4$. The present results demonstrate that the 12-eV satellite is a common effect for all of the 2:1:4 Cu-O systems, as expected. We can identify this d^8 feature for $YBa_2Cu_3O_{6.9}$ at 12.4 eV because Cu 3*p*-3*d* resonance photoemission studies have enhanced it relative to the overlapping Ba 5*p* emission. It has not yet been identified for the Nd and Gd 1:2:3 compounds because the overlapping Ba 5*p* emission obscures it in XPS and resonance studies have not been performed; it can be expected to appear near 12 eV.

In each of the XPS valence-band spectra of Figs. 1 and 2, we have identified a feature at ~9 eV, labeled *B*. It is relatively small at XPS energies, but is much more apparent in spectra taken at lower photon energy. Although it has been observed in all but one previous photoemission study of these high-temperature superconductors, its origin has been elusive (see detailed citations in Ref. 1). (Takahashi *et al.*[11] have reported it missing in scraped single crystals of $La_{1.92}Sr_{0.08}CuO_4$.) In early studies using samples containing substantial amounts of carbon, it was associated with C 2*s* emission. As carbon-free samples were prepared, however, its magnitude diminished, but it has (almost) never vanished. Our studies of carbon-free samples[1] (as verified by the absence of C 1*s* emission in XPS spectra) and those of Stoffel *et al.*[12] indicate that it is an intrinsic part of the excitation spectrum of the superconductor. The fact that it appears for systems where only Cu and O are common argues that it must be related to either Cu or O.

Resonance photoemission studies using Cu 3*p*-3*d* enhancement techniques have shown that there is no increase of the 9-eV structure for $YBa_2Cu_3O_x$ or $(La_{1-x}Sr_x)_2CuO_4$ (Refs. 3, 13, and 14). Our own resonance investigations of the 9-eV structure using single crystals of Pr_2CuO_4 also showed no enhancement associated with the Cu 3*p* core-hole excitation. (Our energy distribution curves and constant-initial-state energy spectra are not shown because they are in general agreement with previous reports.) It is also important to note that interface studies[15] involving overlayers of reactive metals and $YBa_2Cu_3O_{6.9}$ showed that the 9-eV feature persisted even though the 12.4-eV Cu satellite was lost at very low metal coverage (the d^8 satellite vanished by 2 Å of Cu adatom deposition while the 9-eV feature persisted past 6 Å). By elimination, we associate the 9-eV structure with oxygen.

Structure near 9 eV is well known from studies of rare-earth compounds and has been associated with photoemission from OH^- surface radicals. For example, cleaved samples of $CeSi_2$ degrade rapidly to show strong structure at 10 and 6 eV, even at pressures of 5×10^{-11} Torr (Ref. 8). It has been suggested that the 9-eV feature for the high-temperature superconductors might then be due to hydroxyls. Although hydroxyl formation is possible, we have found no evidence for such surface modification. In particular, there was no time dependence of the 9-eV feature, either in XPS or in more surface-sensitive synchrotron radiation measurements, and attempts to enhance the 9-eV feature by exposing clean, cleaved surfaces of Eu_2CuO_4 and $NdBa_2Cu_3O_x$ to ~5000 L (where 1 L = 1 langmuir = 10^{-6} Torr sec) of H_2O at room temperature showed no change. (The reaction with H_2O has been more thoroughly investigated by Qiu *et al.*[16] with condensation of H_2O at 20 K followed by desorption at 300 K. Irreversible changes of the $YBa_2Cu_3O_x$ surface were noted, with a prominent feature at 9.4 eV assigned to an OH_σ orbital and the development of a well-shifted O 1*s* structure.) Again, additional insight is found from Pd and Cu overlayer formation of $YBa_2Cu_3O_{6.9}$ (Ref. 15) where it was found that the 9-eV feature persisted to ~10-Å deposition. If the 9-eV feature were due to hydroxyls, one would expect that adatoms of Cu and Pd would alter the OH signature. We conclude that the 9-eV feature shown here is not related to chemisorption processes, although hydroxyls bonded to the surface would induce emission at that energy.

Finally, the CuO valence-band emission shown at the bottom right of Fig. 3 clearly reveals structure at 10.3, 12.5, and 16.5 eV. This 12-eV satellite is quite pronounced in CuO but much weaker in the high T_c's (compare the reduction in intensity of the 12-eV satellite for CuO vs $La_{1.85}Sr_{0.15}CuO_4$ and $YBa_2Cu_3O_{6.9}$). Its strength in CuO and its close proximity to the energy where feature *B* would appear makes it impossible to argue convincingly that feature *B* exists in CuO. At the same time, its existence cannot be ruled out.

4*f* emission

The superposition of the $La_{1.85}Sr_{0.15}CuO_4$ or $YBa_2Cu_3O_{6.9}$ valence-band spectra with those for the other copper oxides makes it straightforward to identify the 4*f*-derived features (Figs. 1 and 2). Indeed, these

$La_{1.85}Sr_{0.15}CuO_4$ and $YBa_2Cu_3O_{6.9}$ results can be used as reference spectra because the $4f$ states are empty and do not complicate the Cu-O emission (the Ba and La $4f$ emission has been observed in inverse photoemission at 13.5 and 8.7 eV above E_F, respectively[1,17]). Such comparisons have been used routinely to identify $4f$-related photoemission structure in other systems.

From the XPS results for Pr_2CuO_4 and $La_{1.85}Sr_{0.15}CuO_4$ of Fig. 2 it is evident there are *two* distinct $4f$-related features. In Fig. 4 we show these spectra and the difference (shaded region) that results from the subtraction of the reference spectrum ($La_{1.85}Sr_{0.15}CuO_4$ represented by the dashed line). Maxima appear in the difference curve at 1.2 and 4.4 eV, with full widths at half maximum of 0.9 and 1.4 eV, respectively, and much greater strength in the feature nearer E_F. To gain additional evidence that these features were related to $4f$ emission, we collected energy distribution curves at photon energies from 110 to 150 eV using synchrotron radiation, thereby crossing the range of the well-known $4d$-$4f$ resonance.[8] Spectra taken at 110 eV (dashed line, corresponding to off resonance) and 130 eV (solid line, on resonance) are shown in Fig. 4, together with the difference curve. We can again conclude that there are two $4f$-related features, although the results from resonance photoemission indicate broader features because of poorer energy resolution ($\sim$1.2 eV). Finally, a third way of identifying the $4f$ character was also used, namely the measurement of the energy distribution curve at photon energies of 40 and 60 eV. Since the high angular momentum character of the $4f$ electron introduces a delayed onset, the $4f$ emission is enhanced at 60 eV relative to 40 eV. Again, the results reveal two $4f$ features.

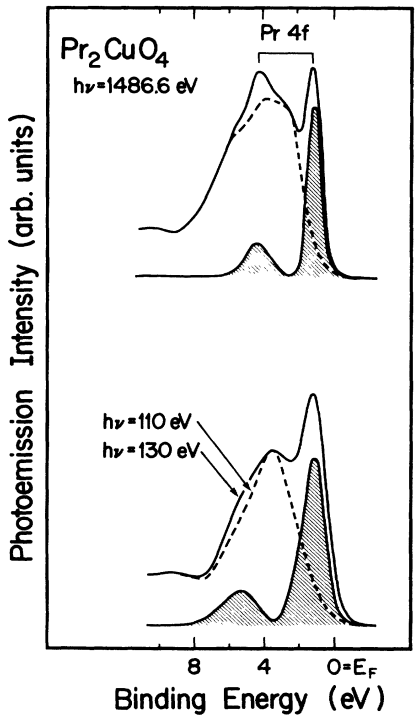

FIG. 4. Comparison of Pr_2CuO_4 photoemission spectra taken on and off resonance (130 and 110 eV, respectively) and (top) XPX results for Pr_2CuO_4 and $La_{1.85}Sr_{0.15}CuO_4$ to reveal the $4f$-derived emission (shaded). These results demonstrate the importance of ligand screening of the $4f$ core hole.

These $4f$ features reflect photoemission final-state effects, analogous to those that were observed for the ionic materials CeP, CeAs, and CeBi.[18] Indeed, similar $4f$-related effects are now familiar from photoemission studies of Ce-based compounds and other light rare-earth compounds.[8] Fujimori and Weaver[19] and Norman, Koelling, and Freeman[20] have discussed the $4f$ excitation spectrum in these correlated systems in terms of two different screening configurations. Fujimori and Weaver modeled the final state by imbedding the emitting atom in a cluster and allowing suitably symmetrized ligand orbitals to provide the screening charge. Norman *et al.* used a supercell to describe f and d final-state screening mediated by the pnictogen p ligand orbitals a few eV below E_F. For PrSb, Norman *et al.* predicted f and d screening states at 0.95 and 4.4 eV. From Fig. 1 we can see that the excitation spectrum for Pr_2CuO_4 shows maxima at 1.2 and 4.4 eV, and we conclude that the formalism described by those authors can be applied directly to the high-temperature superconductors, with differences that must reflect O $2p$ ligands and lattice structure effects. The presence of the two $4f$ features gives conclusive evidence for the Pr^{3+} ($4f^2$) configuration in the ground state, with efficient ligand charge-transfer screening, written $L \rightarrow$ Pr $5d$ or $4f$. In turn, this implies adequate mixing of Pr and O wave functions on the Pr site, producing photoemission final states which are counterparts to those in the ionic material PrSb. For these final states, we note that the ligand atoms involved in screening are not likely to be the oxygen atoms from the Cu-O planes but rather the oxygen atoms which form the ionic Pr-O planes which separate the Cu-O planes (termed off-plane oxygen).

The XPS results of Fig. 1 for $NdBa_2Cu_3O_x$ also show two $4f$ final states at approximately 2.7 and 5.2 eV. They are weaker than for Pr_2CuO_4 because of the proportional reduction in the rare-earth content of the lattice ($\sim$7 vs $\sim$28 at.%), though Nd has one $4f$ electron more than Pr, and the accuracy with which they can be identified is less for $NdBa_2Cu_3O_x$. At the same time, the screening should be analogous, again with subtleties reflecting environmental differences for the Pr and Nd ions in the 1:2:3 and 2:1:4 lattices. Again, Norman *et al.* calculated an excitation spectrum for NdSb with structure at 2.95 and 5.75 eV (versus 2.7 and 5.2 eV for $NdBa_2Cu_3O_x$). Finally, the present experiments for the Pr_2CuO_4 and $NdBa_2Cu_3O_x$ show that the separation in energy of the two $4f$ final states does not track with atomic number, an effect also predicted by Norman *et al.* for PrSb and NdSb.

For Eu_2CuO_4, there is dominant $4f$ emission centered at 5 eV with a shoulder near $\sim$6.5 eV and, probably, another overlapping with feature *B* (Fig. 2). Since Eu forms divalent, trivalent, and mixed-valent compounds, we have compared our XPS results to those from the literature.[21] For divalent Eu in EuO with $4f^7$ configuration, there is dominant $4f$ emission at $\sim$2 eV. For trivalent Eu in Eu_2O_3 with $4f^6$ configuration, the $4f$ multiplet state emission occurs between 4 and 8 eV. We

conclude that Eu is in a 3+ state in the superconductor, as needed for formal charge balance in the formula unit $(Eu_2)^{6+}(CuO_4)^{6-}$.

Finally, the results of Fig. 1 for Gd in these ceramic structures show strong $4f$ multiplet emission peaking at 6 eV for the 2:1:4 and 6.7 eV for the 1:2:3, with relative intensities which scale with the amount of Gd in the compound and increased in energy in the 1:2:3 structure. This energy shift probably reflects differences in atomic environment since Gd is coordinated with oxygen in the 2:1:4 structure but is intercalated between Cu-O planes in the 1:2:3 structure.

O 1s emission

In Fig. 5 we show the O 1s core-level spectra for the 2:1:4 (left) and 1:2:3 (right) superconducting oxides, with all energies referenced to E_F. Inspection reveals a dominant O 1s maximum at -529-eV binding energy and a shoulder at -531 eV (dashed line). This high-energy shoulder is not observed for $La_{1.85}Sr_{0.15}CuO_4$, but the line-shape asymmetry suggests the existence of another component. Moreover, the width of the main line is substantially larger than expected for a single chemical environment, suggesting the existence of two inequivalent O sites in the lattice [1.5 eV full width at half maximum (FWHM) for $La_{1.85}Sr_{0.15}CuO_4$].

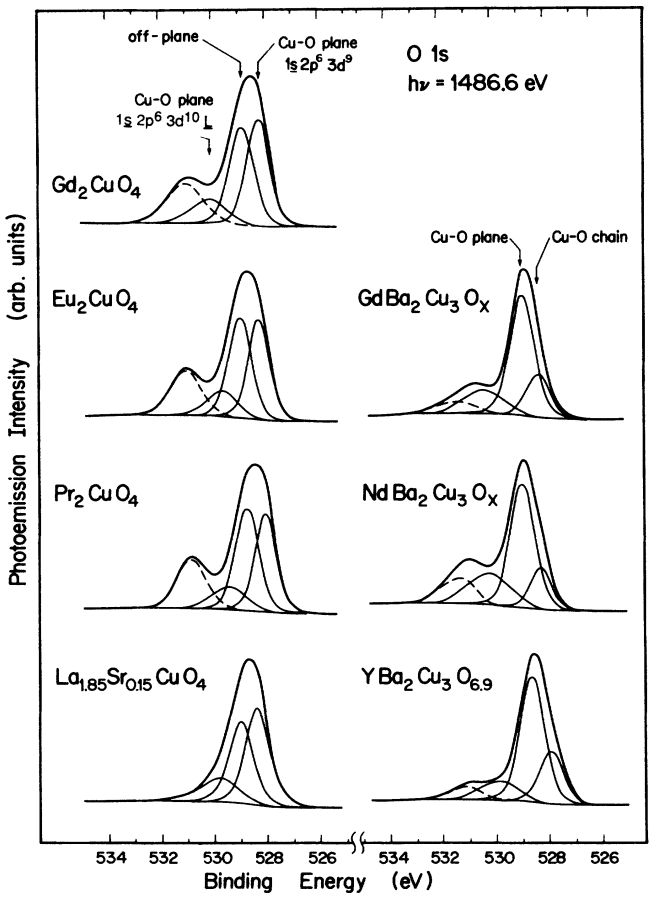

FIG. 5. O 1s core-level spectra analogous to those of Fig. 3. In all cases, two components of approximately equal intensity are found for the 2:1:4 compounds (planes and off planes as identified). For the 1:2:3 compounds, the emission from oxygen in the Cu-O planes dominates that from chains. For the single crystals, it is probable that part of the emission at -531 eV is due to contamination, as discussed in the text, and the fittings to reveal the satellite structure are only qualitative.

In order to be more quantitative in the identification of these two sites, we examined the O 1s emission for CuO and used that line shape to fit the 1s emission for the superconductors. At the left of Fig. 3, we compare the O 1s emission of CuO, $La_{1.85}Sr_{0.15}CuO_4$, and $YBa_2Cu_3O_{6.9}$ with the CuO spectrum offset by 1.15 eV to align the O emission. This offset reflects differences in charge distribution and the tendency toward planar bonding in the superconductor (the binding energy in CuO is greater by 1.15 eV). As shown for CuO, there is a distinct O 1s asymmetry at higher binding energy, indicating the existence of a second component shifted -1.5 eV from the main line (main line FWHM is 1.0 eV). This main-line–satellite structure can be understood in terms of the ground state $3d^9$ and $3d^{10}\underline{L}$ configurations where the O 1s hole is screened by O $2p^6$ electrons. This is analogous to what is observed in the Cu $2p_{3/2}$ spectrum, namely a main line derived from $2\underline{p}_{3/2}3d^{10}\underline{L}$ final states and satellites from $2\underline{p}_{3/2}3d^9$ final-state multiplets. On the other hand, we associate the O 1s main line with $(O\ 1\underline{s}2p^6)3d^9$ and the satellite with $(O\ 1\underline{s}2p^6)3d^{10}\underline{L}$. Following Wendin,[4] we write the ground-state configuration as $[a\,|\,3d^{10}\underline{L}\rangle + b\,|\,3d^9\rangle]$, where the coefficients a and b can be determined approximately by the intensities of the O 1s lines, namely $a^2/b^2 = |\,\text{satellite/main}\,|^2$. With the fits of Fig. 3 for CuO, we estimate that $a^2/b^2 = 0.18$.

Detailed line-shape analysis of the O 1s emission for the superconductors, based on the 1s emission in CuO, yields two components separated by 0.61 eV for $La_{1.85}Sr_{0.15}CuO_4$ and 0.71 eV for $YBa_2Cu_3O_{6.9}$. For $La_{1.85}Sr_{0.15}CuO_4$, the two components have approximately equal strengths, as expected because the crystal structure exhibits equal numbers of planar and off-planar oxygen sites. For $YBa_2Cu_3O_{6.9}$, the central feature is substantially stronger. These fits also produce the small structure at 529.8 eV for $La_{1.85}Sr_{0.15}CuO_4$ and 529.6 eV for $YBa_2Cu_3O_{6.9}$ (Fig. 3) which we associate with the $(O\ 1\underline{s}2p^6)3d^{10}\underline{L}$ satellite.

There are several ways to identify which of the O 1s main lines is associated with the planes and which is associated with the off-plane oxygen in the 2:1:4 structure. First, the satellite structure must be associated with planar Cu–O bonding (off-plane bonding is with the rare earth). The energy separation of the satellite from the large O 1s structures then indicates that the shallower of the two is related to Cu-O planes. Second, evidence that the shallower feature in the 2:1:4 structure is due to Cu-O planes can be found by examining the sensitivity of the Cu $2p$ and O 1s features to degradation. Surface modification (next section) leads to the loss of Cu $2p$ satellite emission (conversion from a formal Cu^{2+} configuration to Cu^{1+}) and a reduction in emission from the shallower O 1s feature, consistent with it being associated with planar oxygen.

For the 1:2:3 compounds, the O 1s line shape is sub-

stantially different from that of the 2:1:4's. To obtain the decompositions shown in Figs. 3 and 5, we again used the spectrum for CuO as the model. The result is two components where the shallower feature is smaller and the overall line shape is narrower. (Overall O 1*s* FWHM was 1.55 eV for Gd_2CuO_4 and 1.23 eV for $NdBa_2Cu_3O_x$.) These changes can be qualitatively understood by examining the 1:2:3 crystal structure. Within the unit cell there are two Cu-O planes in which O atoms are fourfold coordinated with other oxygen atoms (they are slightly inequivalent in the orthorhombic form because the unit-cell dimension is $\sim 1.6\%$ larger along *a* than *b*). These account for four of the seven oxygen atoms in the 1:2:3:7 formula unit. There are then at most three oxygen atoms in chains, with some of these atoms being fourfold coordinated with O and some only twofold coordinated. We propose, therefore, that the dominant O 1*s* feature represents oxygen atoms from the planes and the smaller component reflects oxygen in the chains. Redinger *et al.*[6] have predicted this same hierarchy with O in the planes being more strongly bound than those in the chains.

It is interesting to note that the feature associated with the Cu-O planes is the lower binding energy structure for the 2:1:4's but is the higher binding energy feature for the 1:2:3's. This can be understood by noting that 1:2:3 compounds have Cu-O planes which sandwich a sheet of Y atoms, free of oxygen. In contrast, the 2:1:4 planes are coordinated above and below with rare-earth–oxygen layers. In effect, the planes in the 1:2:3's have intercalated a highly electropositive element and the O 1*s* electrons become more tightly bound. We conclude that the O 1*s* binding energies decrease on going from Cu_2O to CuO to the planes and then to the chains in the superconductors. At the same time, these results show that the absolute binding energy for O in the Cu-O planes of the 1:2:3's is greater than that of O in the Cu-O planes of the 2:1:4's.

The analysis summarized in Figs. 3 and 5 also indicates the persistence of the $(O\ 1\underline{s}2p^6)3d^{10}\underline{L}$ structure. This can be seen best for CuO and $La_{1.85}Sr_{0.15}CuO_4$ (Fig. 3) but is obscured for $YBa_2Cu_3O_{6.9}$ because of a more extensive tailing of the O 1*s* emission. We associate this high-energy tail with emission from contamination[1] and note that it makes decompositions less unique. With that caution, we estimate the main line to satellite intensities, finding $a^2/b^2=0.38$ for $La_{1.85}Sr_{0.15}CuO_4$ and 0.40 for $YBa_2Cu_3O_{6.9}$, compared to 0.18 for CuO. This indicates that the mixing in the ground state for the superconductors is weighted less heavily toward $3d^9$ than for CuO. For the other superconductors, we can infer that the satellite persists, but line-shape analysis is not unique because of the emission at ~ 531 eV (dashed line in Fig. 5) and the intensities are only estimates. They should not be used to determine the *d* count of the Cu atoms. Likewise, it is not possible to determine whether there is a satellite structure associated with the chains in the $YBa_2Cu_3O_{6.9}$ structures (it would overlap the other emission).

As can be inferred from the above, surface contamination has been a particularly serious problem in spectroscopic studies of the high-temperature superconductors. Examination of the literature shows a great deal of variation in the O 1*s* line shape, with some authors showing spectra in which the ~ 531-eV feature dominates.[22] To our knowledge, the only results that are contamination free are ours for polycrystalline $La_{1.85}Sr_{0.15}CuO_4$ (Ref. 23) and those of Takehashi *et al.*[11] for scraped single crystals of $La_{1.92}Sr_{0.08}CuO_4$. Their results and ours indicate that contamination grows at ~ 531 eV. In a recent comparison of a variety of sintered samples of $YBa_2Cu_3O_{6.9}$, we showed that the 531-eV feature diminished as the samples became more effectively sintered, as judged by scanning electron microscopy.[1] For the best samples, fracturing exposed a minimum of the intergranular phase responsible for the feature at 531 eV. The Ba 5*p* spectral features also sharpened with improved sample quality and a significant amount of emission at 4–5 eV in the valence band vanished, giving the spectrum shown in Fig. 1.

The presence of what we assume is a contamination feature is noted by the dashed lines of Fig. 5. Its persistence is disturbing for single crystals, but it can probably be understood in terms of flux incorporation during crystal growth from the melt, as well as intercalation during processing or storage. Internal weakening would facilitate cleaving or fracturing to expose the second component. Its presence in photoemission spectra for cleaved single crystals indicates that characterization of these surfaces should be done in concert with XPS. Certainly, the overlap of a contamination feature with the $(O\ 1\underline{s}2p^6)3d^{10}\underline{L}$ satellite encourages caution in quantitative discussions.

Surface degradation

Degradation of $(La_{1-x}Sr_x)_2CuO_4$ due to reaction in vacuum with residual gasses has been reported by Hill *et al.* (Fig. 1 of Ref. 23) and again by Takahashi *et al.*[11] Both studies have shown an increase in O 1*s* emission at 531 eV, and Hill *et al.* found negligible changes in Cu 2*p* emission. They associated the spectral changes to chemisorption with minimal modification of the substrate. Internal degradation of these samples can also occur over time in air. To demonstrate this, we fractured a bulk sample of $La_{1.85}Sr_{0.15}CuO_4$ that had been characterized shortly after it had been synthesized (the spectra of Fig. 5). As a result of aging in a dessicator for nine months, the O 1*s* emission at 531 eV grew and there was a broadening of the Cu 2*p* emission. There was no parallel buildup of C 1*s* emission, indicating that the 531-eV peak for $La_{1.85}Sr_{0.15}CuO_4$ reflects reaction with O_2, or some other oxygen-containing molecule. For single crystals, this internal degradation should be much smaller because of the greater structural integrity compared to sintered polycrystals but it may be non-negligible.

It was noted above that time dependences were sometimes observed in the Cu 2*p* and O 1*s* emission that indicated modification of the sample surface, but that these changes were different from those associated with chemisorption. In Fig. 6 we show the Cu $2p_{3/2}$ and O 1*s* emission for Gd_2CuO_4 and Eu_2CuO_4 single crystals where the solid curves were obtained within 15 min of cleaving, the dashed curve corresponds to aging for 5 h at a pressure of 1×10^{-10} Torr, and the shaded areas represent the

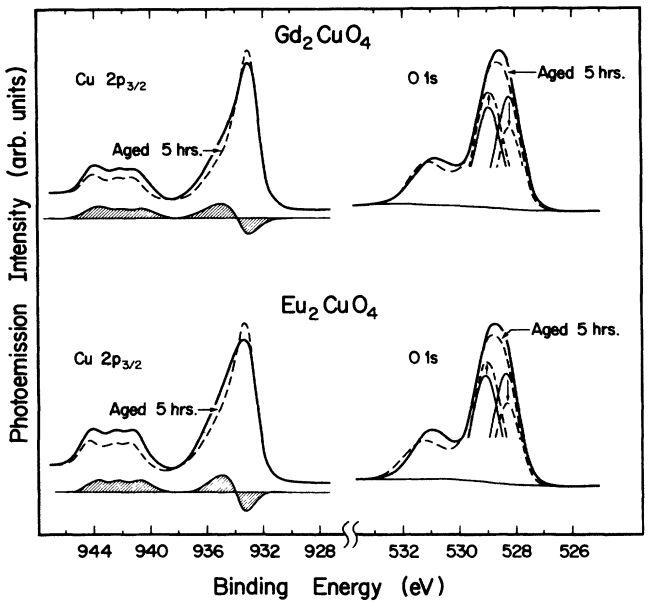

FIG. 6. Time-dependent Cu $2p_{3/2}$ and O $1s$ spectra for single crystals of Gd_2CuO_4 and Eu_2CuO_4 showing the loss of the Cu satellite and the reduction in the O-in-planes emission. We attribute these changes to the redistribution or loss of oxygen in the near-surface region. As emphasized in the text, such effects were observed in three of the 11 cleaves and are probably due to structural instabilities following cleavage. The worst-case results emphasize that cleaved single crystals can exhibit time dependences.

differences. These changes were not induced by the x-ray beam, as verified by examining different spots on the sample. The effect of aging was the loss in the Cu $2p$ satellite intensity and a sharpening of the main line due to conversion from formal Cu^{2+} to Cu^{1+}. This is accompanied by a loss in intensity for the in-plane Cu-O main line and the growth of emission from "other" oxygen bonding configurations, as can be seen by comparing the solid and dashed spectra at the right of Fig. 6.

The changes implied by Fig. 6 are due to the loss or redistribution of oxygen in the outermost layer(s) of the sample, resulting in disorder and a modification of the surface structure. On the one hand, it is likely that this surface region would not be superconducting, as inferred from the changes in Cu $2p$ and O $1s$ emission. (Although our single crystals were semiconductors, the Cu $2p$ line shape is the same for the superconductors studied and changes from 2+ to 1+ have been observed during surface disruption, as discussed in Refs. 1 and 15, for example.) On the other hand, such changes will be reflected in the energy bands of the solid, with disorder-induced broadening of the bands derived from wave functions which are sensitive to this disorder, and more substantial changes associated with structural modification. Angle-resolved photoemission and inverse photoemission studies that seek to probe the details of the bands would be troubled by such surface effects. The possibility of surface changes would indicate that such studies should be undertaken in conjunction with XPS to assess chemical stability and low-energy electron diffraction as an important gauge of structural stability.

We emphasize that changes of the sort shown in Fig. 6 were not always observed and, in most cases, there were no changes at all. Of the 11 cleaves of the single crystals examined, only three showed changes like those of Fig. 6. The results shown in Figs. 1–5 were obtained with samples which had no time dependences.

We speculate that surface stability reflects the detailed atomic distribution that results from cleaving and/or fracturing. For these ceramics, it is likely that a cleaved surface with a nearly perfect termination would be more stable than one fractured across the grain. Indeed, we have found that it was possible to observe sharp low-energy electron diffraction patterns that were stable over many hours for single crystals of Gd_2CuO_4. For less ideal surfaces, or portions of surfaces, we suspect that substantial atomic relaxation might occur, the local energetics and Cu–O bonding configurations could change, and the structure could be altered.

SUMMARY

In this paper, we have shown that the valence bands of the 1:2:3 and 2:1:4 structures are all very similar, reflecting dominant emission from Cu $3d$ and O $2p$ states. We have shown that the formation of Pr-O and Nd-O layers in the 2:1:4 structures gives rise to $4f$ final-state effects that are well described by ligand screening models and calculations. In all cases, we have observed a feature at -9 eV but its origin is unknown. Studies of the rare-earth $5p$ core levels suggest complex $5p$-$4f$ multiplet states. Studies of the O $1s$ core levels distinguished emission from oxygen atoms in the Cu-O planes and chains for the 1:2:3's and the Cu-O planes and off-planes for the 2:1:4's. Emission from the Cu-O planes is characterized by a main line and a weak satellite, reflecting $(O\ 1\underline{s}2p^6)3d^9$ and $(O\ 1\underline{s}2p^6)3d^{10}\underline{L}$, respectively. The relative intensity of these features was used to determine the ground-state weighting for CuO, $La_{1.85}Sr_{0.15}CuO_4$, and $YBa_2Cu_3O_{6.9}$. The overlap of the satellite with a feature which is likely to be related to contamination (531-eV O $1s$ feature) prevented detailed analysis for the other samples.

Based on our results, we caution that the cleaving of these ceramic single crystals produces a surface which is not well understood. As a result, surface spectroscopies may not be as free of spurious effects as we would like, particularly when the photon or electron beam probes a large surface. This situation will doubtless change as sample synthesis is perfected and a wide variety of surface studies provide insight into the character of the surface.

ACKNOWLEDGMENTS

It is a pleasure to acknowledge stimulating discussions with G. Wendin, A. Fujimori, and N. G. Stoffel. The single crystals of CuO were generously provided by C. Gallo. I. M. Vitomirov and G. D. Waddill contributed to the synchrotron radiation photoemission experiments (performed at the National Science Foundation-supported Aladdin

facility at the Wisconsin Synchrotron Radiation Center). The work at the University of Minnesota was supported by the Office of Naval Research under Contract No. ONR N0014-87-K-0029. The work at Los Alamos National Laboratory was supported by the Department of Energy.

[1]An exhaustive list of previous experimental and theoretical results for 2:1:4- and 1:2:3-type superconductors can be found in H. M. Meyer III, D. M. Hill, T. J. Wagener, Y. Gao, J. H. Weaver, D. W. Capone II, and K. C. Goretta, Phys. Rev. B (to be published). The cumulative number of papers is now very large.

[2]A. Fujimori, E. Takayama-Muromachi, Y. Uchida, and B. Okai, Phys. Rev. B **35**, 8814 (1987).

[3]Z. Shen, J. W. Allen, J. J. Yeh, J. S. Kang, W. Ellis, W. Spicer, I. Lindau, M. B. Maple, Y. D. Dalichaouch, M. S. Torikachvili, J. Z. Sun, and T. H. Geballe, Phys. Rev. B **36**, 8414 (1987).

[4]G. Wendin, *Proceedings of the 14th International Conference X-Ray and Inner-Shell Processes* [J. Phys. (Paris) (to be published)].

[5]L. F. Mattheiss, Phys. Rev. Lett. **58**, 1028 (1987); L. F. Mattheiss and D. R. Hamann, Solid State Commun. **63**, 395 (1987); F. Herman, R. V. Kasowski, and W. Y. Hsu, Phys. Rev. B **36**, 6904 (1987); W. M. Temmerman, G. M. Stocks, P. J. Durham, and P. A. Sterne, J. Phys. F **17**, L135 (1987); D. W. Bullett and W. G. Dawson, J. Phys. C **20**, L853 (1987); B. A. Richert and R. E. Allen, Phys. Rev. B **37**, 7869 (1988); T. Fujiwara and Y. Hatsugai, Jpn. J. Appl. Phys. **26**, L716 (1987); T. C. Leung, X. W. Wang, and B. N. Harmon, Phys. Rev. B **37**, 384 (1988).

[6]J. Redinger, J. Yu, A. J. Freeman, and P. Weinberger, Phys. Lett. A **124**, 463 (1987); J. Redinger, A. J. Freeman, J. Yu, and S. Massidda, *ibid.* **124**, 469 (1987).

[7]See, for example, *Photoemission in Solids II,* edited by L. Ley and M. Cardona, Topics in Applied Physics, Vol. 27 (Springer-Verlag, New York, 1979).

[8]*Handbook on the Physics and Chemistry of Rare Earths, Vol. 10,* edited by K. A. Gschneider, Jr., L. Eyring, and S. Hufner (North-Holland, Amsterdam, 1987) provides an excellent, up-to-date review of high-energy spectroscopies of the rare earths. Synchrotron radiation photoemission studies are discussed in Chap. 66 by D. W. Lynch and J. H. Weaver.

[9]M. R. Thuler, R. L. Benbow, and Z. Hurych, Phys. Rev. B **26**, 669 (1982).

[10]G. van der Laan, C. Westra, C. Haas, and G. A. Sawatsky, Phys. Rev. B **23**, 4369 (1981).

[11]T. Takahashi, F. Maeda, H. Katayama-Yoshida, Y. Okabe, T. Suzuki, A. Fujimori, S. Hosoyo, S. Shamato, and M. Soto, Phys. Rev. B **37**, 9788 (1988). Single-crystal studies for $La_{1.92}Sr_{0.08}CuO_4$.

[12]N. G. Stoffel, Y. Chang, M. K. Kelly, L. Dottl, M. O'Nellion, P. A. Morris, W. A. Bonner, and G. Margaritondo, Phys. Rev. B **37**, 7952 (1988) discusses angle-resolved photoemission of $YBa_2Cu_3O_x$.

[13]R. L. Kurtz, R. L. Stockbauer, D. Mueller, A. Shih, L. E. Toth, M. Osofsky, and S. A. Wolf, Phys. Rev. B **36**, 8818 (1987).

[14]M. Onellion, Y. Chang, D. W. Niles, R. Joynt, G. Margaritondo, N. G. Stoffel, and J. M. Tarascon, Phys. Rev. B **36**, 819 (1987).

[15]T. J. Wagener, Y. Gao, I. M. Vitomirov, C. M. Aldao, J. J. Joyce, C. Capasso, J. H. Weaver, and D. W. Capone II, Phys. Rev. B **38**, 232 (1988). Noble and near-noble metal overlayer formation on $YBa_2Cu_3O_{6.9}$.

[16]S. L. Qiu, M. W. Ruckman, N. B. Brooks, P. D. Johnson, J. Chen, C. L. Lin, M. Strongin, B. Sinkovic, J. E. Crow, and C. S. Lee, Phys. Rev. B **37**, 3747 (1988). For an exhaustive review of the interaction of H_2O with surfaces, see P. A. Thiel and T. E. Madey, Surf. Sci. Rep. **7**, 211 (1987). R. L. Kurtz, R. Stockbauer, T. E. Madey, D. Mueller, A. Shih, and L. E. Toth, Phys. Rev. B **37**, 7936 (1988) communicate that they have observed the growth of OH-related features at $\sim$5 eV and $\sim$9 eV during H_2O exposure at room temperature, and that the deeper feature is shifted relative to that observed for the freshly prepared surface of $La_{2-x}Sr_xCuO_4$.

[17]T. J. Wagener, Y. Gao, J. H. Weaver, A. J. Arko, B. K. Flandermeyer, and D. W. Capone II, Phys. Rev. B **36**, 3899 (1987); Y. Gao, T. J. Wagener, J. H. Weaver, B. K. Flandermeyer, and D. W. Capone II, *ibid.* **36**, 3971 (1987).

[18]A. Franciosi, J. H. Weaver, N. Mårtensson, and M. Croft, Phys. Rev. B **24**, 3651 (1981).

[19]A. Fujimori and J. H. Weaver, Phys. Rev. B **31**, 6345 (1985).

[20]M. R. Norman, D. D. Koelling, and A. J. Freeman, Phys. Rev. B **32**, 7748 (1985).

[21]J. Barth, F. Gerken, J. Schmidt-May, A. Flodström, and L. I. Johansson, Chem. Phys. Lett. **9**, 532 (1983).

[22]D. D. Sarma, K. Sreedhur, P. Ganguly, and C. N. R. Rao, Phys. Rev. B **36**, 2371 (1987).

[23]D. M. Hill, H. M. Meyer III, J. H. Weaver, B. K. Flandermeyer, and D. W. Capone II, Phys. Rev. B **36**, 3979 (1987).